Journal of Alloys and Compounds 892 (2021) 162043

Contents lists available at ScienceDirect

Journal of Alloys and Compounds

journal homepage: www.elsevier.com/locate/jalcom

Mechanical behavior of the HfNbZrTi high entropy alloy after ion irradiation based on micro-pillar compression tests

Shengyuan Peng[a], Ke Jin[b,*], Xin Yi[c], Zhaohui Dong[c], Xun Guo[a], Ying Liu[c], Yangyang Cheng[c], Nannan Jia[b], Huiling Duan[c], Jianming Xue[a,c,**]

[a] State Key Laboratory of Nuclear Physics and Technology, School of Physics, Peking University, Beijing 100871, PR China
[b] Advance Research Institute of Multidisciplinary Science, Beijing Institute of Technology, Beijing 100081, PR China
[c] State Key Laboratory for Turbulence and Complex Systems, Department of Mechanics and Engineering Science, BIC-ESAT, Peking University, Beijing 100871, PR China

ARTICLE INFO

Article history:
Received 2 July 2021
Received in revised form 4 September 2021
Accepted 17 September 2021
Available online 21 September 2021

Keywords:
High entropy alloy
Irradiation
Micropillar compression

ABSTRACT

High entropy alloys (HEAs) have exhibited excellent irradiation resistance regarding structure stability. However, limited knowledge has been available on the tendency of mechanical properties of HEAs with body-centered cubic structures after ion irradiation. In this study, the evolution of mechanical properties of the HfNbZrTi irradiated with 3 MeV C ions is studied based on micropillar compression tests. The yield strength increases almost linearly from 974 to 2068 MPa with increasing irradiation doses up to 0.98 dpa. The correlation between the mechanical and microstructural changes agrees well with the prediction of $\Delta\delta_y = \alpha MGb(ND)^{\frac{1}{2}}$, indicating a similar strengthening mechanism with conventional alloys. Nonetheless, the irradiation strengthening effect in this alloy is less pronounced in the low dose regime, and the saturation is postponed, compared with the stainless steel and the 3d metal high entropy alloys with face-centered cubic structures, exhibiting promising irradiation resistance regarding mechanical properties.

1. Introduction

Next-generation nuclear power plants demand novel structural materials with enhanced properties against the extreme service environment in the reactors[1]. The recent development of high entropy alloys (HEAs) has greatly broadened the alloy composition space of interest, and provided a new alloy design strategy on tuning the intrinsic disorders at the atomic level. Moreover, this novel family of alloys have been demonstrated to have outstanding properties on irradiation tolerance, strength-ductility trade-off, corrosion resistance, etc., which grant them potential applications as one of the next-generation nuclear structural materials.[2–5–8].

The irradiation effects have been extensively investigated in the HEAs, but majority of these works focused on the irradiation induced microstructural evolution and phase stability [9–12,13]. For example, the Fe-Ni-Mn-Cr HEA did not exhibit any phase instability after ion irradiation up to midrange doses of 10 dpa [12]. Another recent study on $Al_xCoCrFeNi$ HEA has reported better phase stability than conventional nuclear materials [10]. Since irradiated high entropy alloys exhibit good resistance to excellent phase stability. However, the understanding on the degradation of mechanical properties of HEAs under irradiation, which is fundamental and important for applications, remains limited. For the HEAs, which has gained increasing attention recently due to their outstanding high-temperature properties and relatively low neutron activity [4,9,14], quantitative analyses on the irradiation-induced strengthening, i.e., the change in the yield strength as a function of irradiation dose, remains largely unknown. In general, the lack of studies on the mechanical property change for ion irradiated materials is mostly due to the challenge from the shallow damage range.

Most previous works on studying irradiation induced strengthening in HEAs are based on nanoindentation techniques for the ion irradiated samples [15–17,14,3,13]. For examples, Chen et al. utilized nanoindentation to compare the irradiation hardening between the HEAs and stainless steels [14]. However, this technique faces various issues, such as the indentation size-effects, and the high sensitivity to surface states, which bring difficulties to proper correlation between the indentation hardness and the bulk mechanical properties [14,15,18,19]. As an emerging technique, the in situ micropillar compression test provides an alternative way to investigate the mechanical properties of the

* Corresponding author.
** Corresponding author at: State Key Laboratory of Nuclear Physics and Technology, School of Physics, Peking University, Beijing 100871, PR China.
E-mail addresses: jinke@bit.edu.cn (K. Jin), jmxue@pku.edu.cn (J. Xue).

https://doi.org/10.1016/j.jallcom.2021.162043
0925-8388/

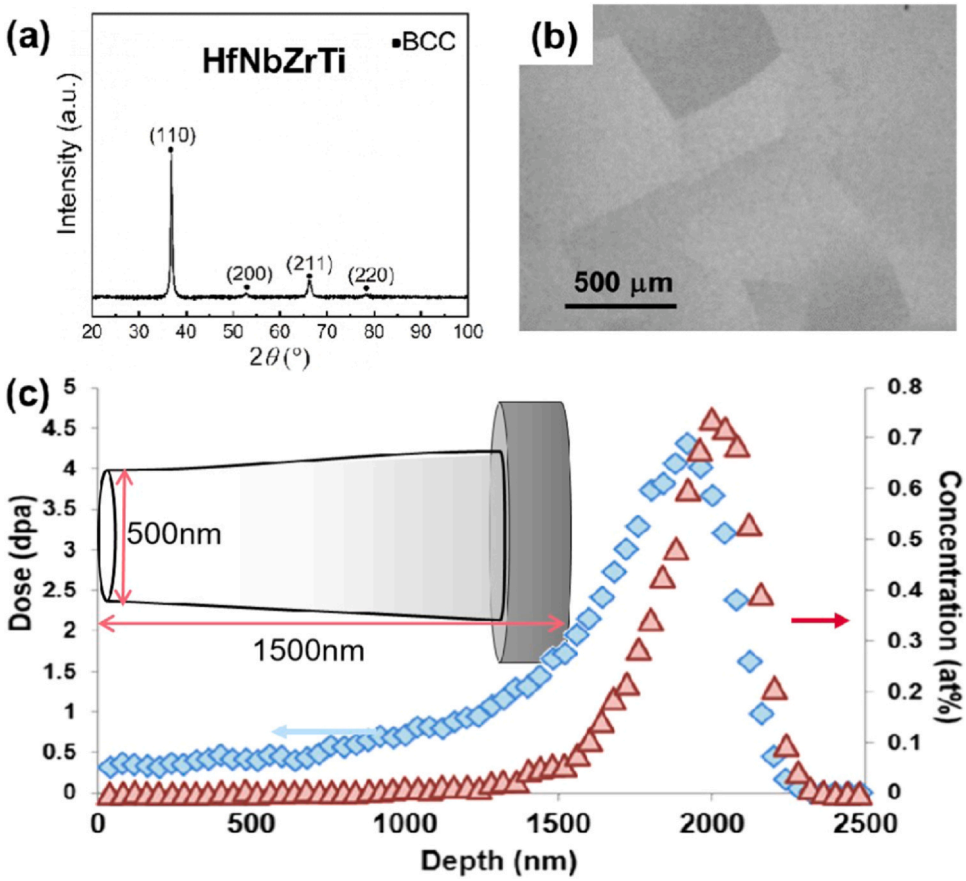

Fig. 1. (a) XRD patterns and (b) SEM-BSE images of the as prepared HfNbZrTi alloy. (c) SRIM plots showing the calculated damage (blue) and implanted ion concentration (red). (For interpretation of the references to colour in this figure legend, the reader is referred to the web version of this article.)

shallow damaged region in the ion irradiated materials. Kiener et al. showed that in the single crystalline copper irradiated to 0.8 dpa with proton, the yield strengths are size independent with diameters greater than ∽400 nm [20], which means, to a certain extent, the capability of indicating the bulk properties. Moreover, Shan et al. found that the data obtained with in-situ compression tests can be directly correlated with the dynamic microstructure evolution in the submicrometer-diameter pillars [21]. Regarding the HEAs, Zou et al. has used the micropillar compression tests to identify an HEA with remarkably high yield strength of 8–10 GPa [22]. Recently, Maryam et al. used this method to compare a HfTaTiNiVZr HEA with stainless steel regarding the irradiation hardening, but only one irradiation dose was tested so that the evolution process was not considered [16].

HfNbZrTi is a model high entropy alloy with a single-phase body-centered cubic (BCC) structure and excellent combination between strength and ductility. Here, in order to understand the mechanical changes produced by irradiation on HfNbZrTi alloy, micropillar compression has been employed. In situ micropillar compression tests have been performed in a scanning electron microscope (SEM) to explore the yielding behavior at different radiation doses and compared with conventional nuclear alloys. This work provides the initial understanding of microstructural and mechanical changes produced by irradiation of an HEA material, thereby giving insight into the potential of this family of materials for nuclear applications.

2. Method

The raw metal of Hf, Nb, Zr,and Ti with purities higher than 99.9% were carefully weighted. The alloy button of HfNbZrTi with equiatomic concentration was prepared by arc melting in a Ti-gettered high purity argon atmosphere. In order to enhance homogeneity, the button was flipped and re-melted at least seven times, during which melting process electromagnetic stirring was conducted. The as-cast alloy, sealed in a quartz-tube filled with high purity argon, was homogenized at 1300 °C for 24 h and then water quenched. Subsequently, the homogenized alloy was cold rolled for a thickness reduction of 78%, followed by a recrystallization process at 1300 °C for 24 h.

Ion irradiations were performed at a irradiation facility, the Peking University of State Key Laboratory of Nuclear Physics and Technology. The depth distribution of the damage and the implanted carbon atoms were estimated using the Stopping and Range of Ions in Matter (SRIM) code assuming a displacement energy of 40 eV for all elements and the quick Kinchin-Pease mode [9]. The samples were irradiated with 3 MeV C ions at room temperature, and a low fluence ratio of 1.8×10^{12} cm^{-2} s was used to avoid significant temperature rise. The irradiation fluence ranged from 1.58×10^{15} to 1.42×10^{16} cm^{-2}.

At least five pillars were fabricated for each irradiation dose using the focused ion beam (FIB, FEI-Helios G4) technique at the crystal grains with {111} surfaces, as confirmed using the Electron backscattered diffraction (EBSD). The taper angle measured for each pillar was less than 2°. It is well known that micropillars show strong size effect. However, as shown in Kiner et al's report, the irradiated material exhibits a size-independent yield stress for micropillars diameters larger than 400 nm. Therefore, in this work, the micropillars were fabricated with a diameter of 500 nm and a height of 1500 nm [20].

Conventional X-Ray diffraction measurement were performed on the as-fabricated HfNbZrTi HEA bulk material with a copper tube at

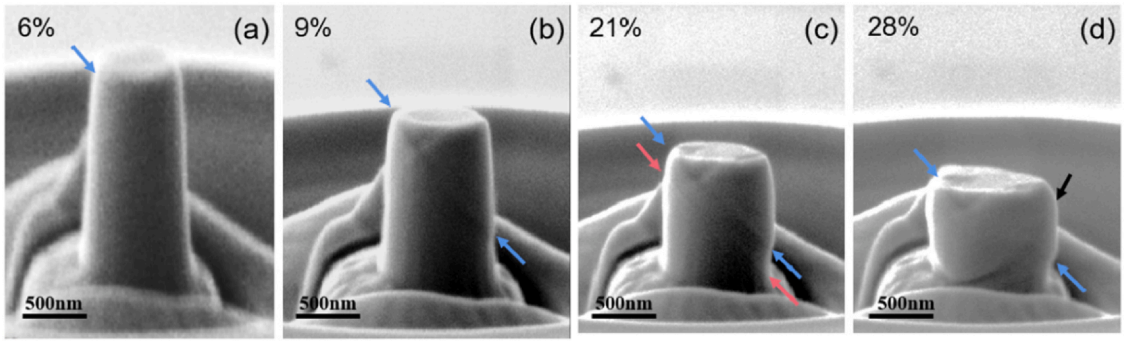

Fig. 2. SEM images of the micropillar compressed to different strain levels. The sample was irradiated to a dose of 0.11 dpa. The arrows pointed on the slip traces.

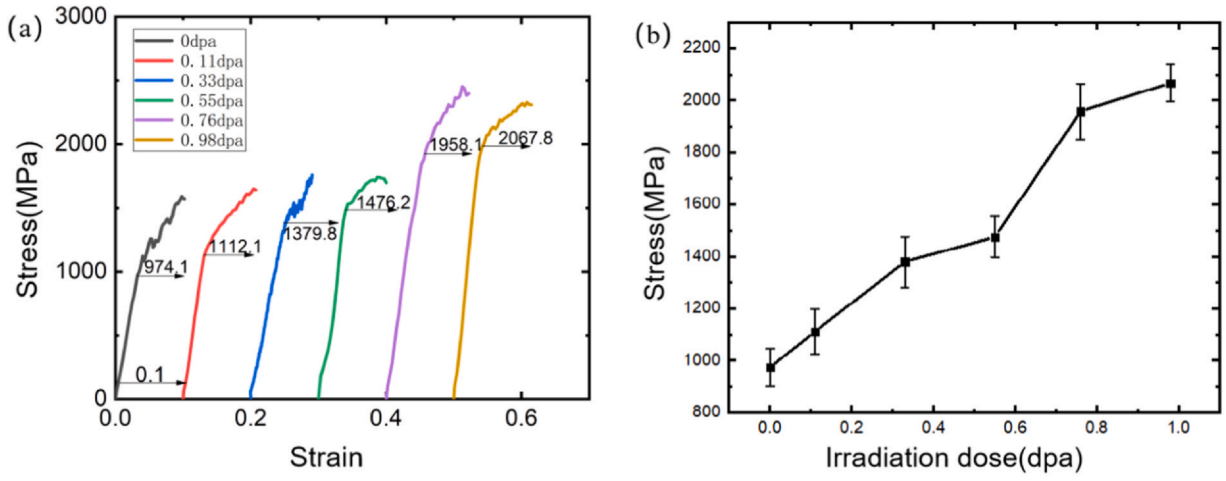

Fig. 3. (a) Representative stress-strain curves of the micropillars irradiated to different doses. (b) Yield strength as a function of irradiation damage.

room temperature at an accelerating voltage and current of 40 kV and 40 mA. Microstructural characterization included scanning electron microscopy (SEM) and transmission electron microscopy (TEM). A MAIA 3 GMU SEM with EBSD detector and a Hitachi SU3800 SEM equipped with a backscatter electron (BSE) detector were performed on the as-fabricated HEAs. The defects in HEAs were analyzed using transmission electronic microscopy (TEM, Tecnai F30). All the samples for TEM analyses were also prepared by using FIB. In order to remove the unwanted FIB damage caused by 30 keV Ga^+, "5 kev 48 pA Ga^+ clearance" was subsequently conducted.

In-situ micropillars tests were performed using a FT-NMT03 test module equipped with an 8 μm flat punch diamond tip at a strain rate of 2×10^{-3} s^{-1} in the displacement control mode. The load-displacement data were converted to engineering stain-stress curves for further analyse. At least three pillars were tested of the samples irradiated at different ion fluence.

As shown in Fig. 1, The XRD spectrum (Fig. 1a) indicates that the HfNbZrTi alloy has a single-phase BCC structure with a lattice constant of ∽0.34 nm, and no secondary phases are observed. Fig. 1b shows that the grains size is several hundreds microns, which is large enough to ensure the fabrication of 5 pillars with 500 nm diameter on the same grain, and the grain boundaries are readily avoided for characterizing both microstructures and mechanical properties. As shown in Fig. 1c the damage peak was located ∽2000 nm from the surface. So that the damage level in the micropillars only slightly varied, and the implanted carbon concentration inside the pillars is negligible. The irradiation doses range from 0.11 to 0.98 dpa at the depth of 1500 nm, corresponding to the average value through the depth of the pillars.

3. Results and discussions

3.1. Slip traces

Fig. 2 shows the SEM images of a compressed micropillar irradiated to 0.11 dpa at different strain levels. According to the angles between the surface and the slip planes characterized from EBSD, the slip traces of $(101)/[11\bar{1}]$ is identified at low strains, as shown in Fig. 2a and b. Another parallel slip trace is observed when the strain increases up to 21% (Fig. 2c). As the strain increases to 28%, $(0\bar{1}1)/[1\bar{1}\bar{1}]$ slips are further activated (Fig. 2d). The deformation is plastic through the localized slips on the preferred glide planes, and the slip traces can be observed across the pillar surface. Such deformation behavior is similar to the dislocation dynamics simulation results [23] and what observed in some BCC metals such as Nb [12].

3.2. Micromechanical properties

Fig. 3a shows the engineering stress-strain curves obtained from the micropillar compression tests of the samples irradiated at different ion fluence. At least three pillars were tested for each condition to obtain the standard deviation. The yield strength in all cases was obtained using the 0.2% strain offset, as shown in Fig. 3b. The average yield strength is increased from 974.1 MPa to 2067.8 MPa with the irradiation dose increased from 0 to 0.98 dpa. The irradiation strengthening has been reported in several HEAs. For example, the increase in yield strength for FeNiMnCr was 35% at an irradiation dose of 0.03 dpa [12]. The present results indicate that the HfNbZrTi HEA has a less pronounced irradiation strengthening effects at low

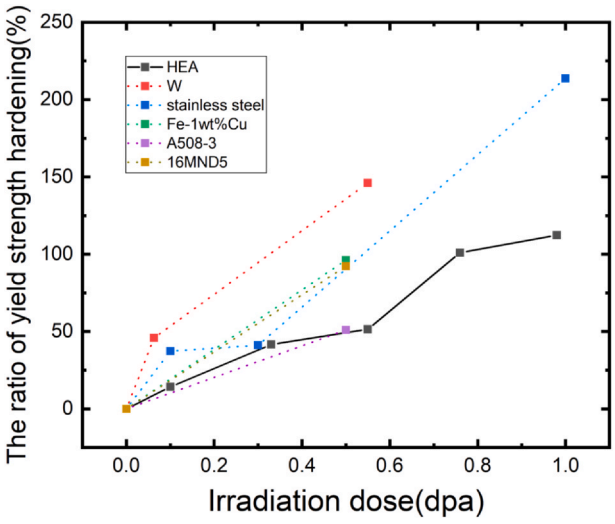

Fig. 4. Effects of ion irradiation dose on yield stress for HfNbZrTi HEA compared with conventional nuclear structural materials.[29–31].

damage level, which agrees to the literature results [16]. It should be noted that, the irradiation strengthening has been reported to saturate in the single-phase FCC NiFe alloy under a relatively low irradiation dose below 0.5 dpa [13,24] but here the irradiation strengthening increases almost linearly with the displacement dose up to at least 1 dpa, indicating a delayed strengthening process in the HEAs. The Young's modulus are also obtained from the stress-strain and are shown in the Supplemental Materials. The Young's modulus ranges from 34 GPa to 50.32 GPa with the irradiation dose increasing to 0.98 dpa. the Young's modulus should not be strongly affected in ion irradiated metals at room temperature, since the dislocation loops are the dominant types of irradiation defects, as shown in previous work [25,26].

Fig. 4 compares the dose-dependent yield strength for the HfNbZrTi with previously conventional nuclear structural materials. Since the yield strength could be crudely estimated from the hardness measurements utilizing an liner equation:

$$YS = kH \tag{1}$$

with yield stress YS in MPa, hardness H in MPa. k is a material-dependent constant, which is taken as 0.31, such parallel comparison should be reasonable [27–30,31].

The irradiation strengthening of HfNbZrTi HEA is significantly lower than 16MND5 steels, A508–3 steels and tungsten [29–31]. For example, as the ion dose increases to 0.5 dpa, the yield stress of Fe-1 wt%Cu alloy and HfNbZrTi alloys increases for 96.2% [31] and 51.5%, respectively. As the ion dose increases to 1 dpa, the HfNbZrTi shows 112.3% hardening, which is much smaller as compared with the value of 213.7% for the stainless steel [30]. Overall, the HfNbZrTi HEA shows outstanding irradiation resistance on mechanical properties.

3.3. Microstructure characterization

In order to understand the mechanism of irradiation-induced strengthening in these alloys, the microstructure of the irradiated alloys was characterized using TEM. Fig. 5 shows the representative cross-sectional TEM images at various depths for the sample irradiated at the doses of 0.11 dpa and 0.55 dpa. It can be observed that, other than the "black dot" defects, most resolvable defect clusters exhibit the feature of dislocation loops.

The density and size of dislocation loops as a function of dpa values are shown in Fig. 6. The size of loops remains almost unchanged with increasing irradiation dose up to 0.98 dpa, but the

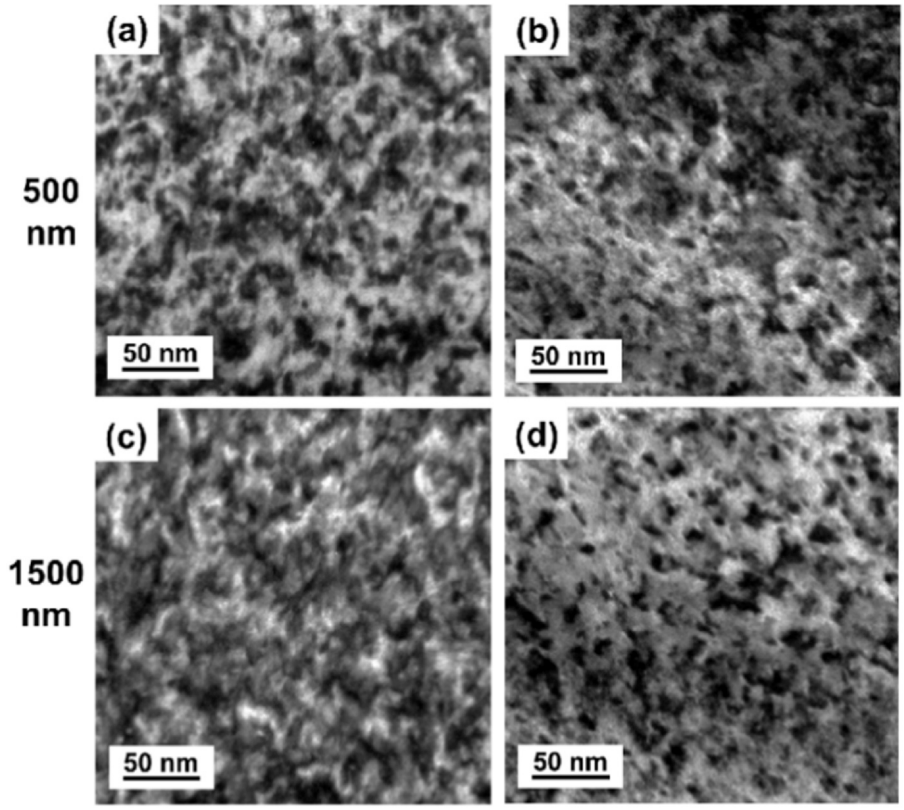

Fig. 5. Cross-sectional TEM images of the HfNbZrTi alloys irradiated with C ions to the dose of (a, c) 0.11 dpa and (b, d) 0.55 dpa, observed under the two-beam condition with a g vector of $[1\bar{1}0]$, taken at (a, b) 500 nm and (c, d) 1500 nm.

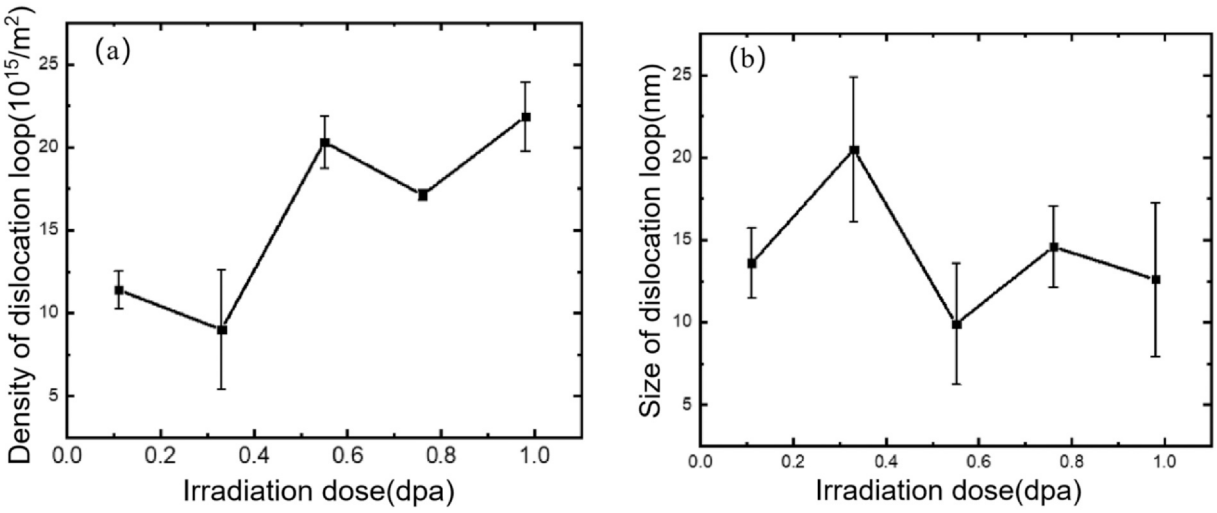

Fig. 6. Evolution of (a) density and (b) size of the irradiation-induced loops as a function of irradiation dose.

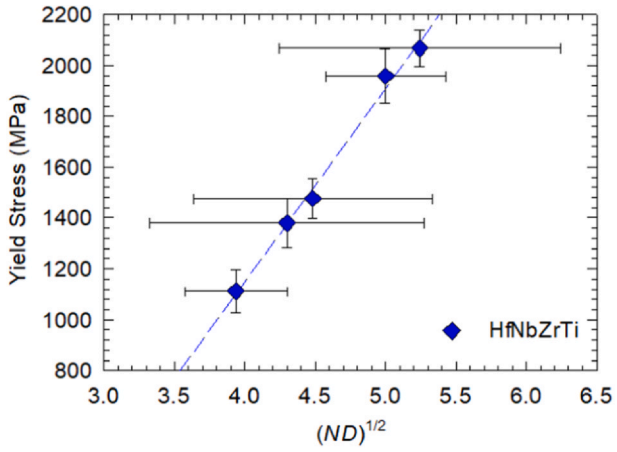

Fig. 7. Correlation between the yield stress and the square root of the product of defect density and size.

defect density is progressively increased as shown in Fig. 6a, and the similar results were also reported in the FeCrAl multi-principal element alloy [32]. The irradiation-induced strengthening is mainly attributed to the increasing defect density. Note that the sizes of irradiation induced dislocation loops in the FCC structured HEAs, such as CoCrMnFeNi and $Al_{0.3}$CoCrFeNi, considerably increase with increasing irradiation dose in this range. Our results suggest that the BCC structured HfNbZrTi HEA may have a more suppressed defect accumulation process. The irradiation induced loop strengthening in metals can be described with a well-established strengthening relationship [12].

$$\Delta\delta_y = \alpha MGb(ND)^{\frac{1}{2}} \quad (2)$$

where M is the Taylor factor, which is 3 for the BCC structure, α is a material dependent constant for the average barrier strength of loops, assumed as 0.4 (for strong obstacles such as dislocation loops) [12], G is the shear modulus, b is the Burgers vector, assumed as 0.254 nm [12], N is the defect density, and D is the defect size. According to the correlation between yield stress and the size and density of loops at different irradiation doses, as plotted in Fig. 7. Although large scattering is shown the data points, the good linear correlation is observed following Eq. (2), demonstrating a typical loop-type irradiation strengthening similar to the conventional alloys.

4. Conclusions

In the present work, the mechanical behavior of the HfNbZrTi high entropy alloy under ion irradiation with doses ranging from 0.11 dpa to 0.98 dpa has been examined. The micro-compression test is based on the mircopillars with dimensions of 500 nm and 1500 nm in diameter and height, respectively. The microstructural characterization correlates the irradiation strengthening to the irradiation-induced dislocation loops. Moreover, the evolution of yield strength in HfNbZrTi high entropy alloy is compared with conventional nuclear materials under similar irradiation dosages. The following can be concluded:

- The yield strength of HfNbZrTi high alloy is increased almost linearly from 974 to 2068 MPa with the dose increased up to 0.98 dpa.
- The radiation-induced defects are mainly dislocation loops.
- The defect density is progressively increased and the size of loops remains almost unchanged with increasing irradiation dose. The irradiation-induced hardening results from the increased radiation defect loops, and generally follows the prediction of DBH model.
- The saturation in the strengthening effect postponed towards higher dose level is because of the suppressed aggregation of defect cluster, as evidenced by the weak coarsening of the loops.
- As compared with the strengthening of several conventional alloys under the similar irradiation doses. HfNbZrTi shows the least strengthening effect, indicating an excellent irradiation resistance on mechanical properties.

CRediT authorship contribution statement

Shengyuan Peng: Methodology, Formal analysis, Writing – review & editing, Data curation, Writing – orignal draft, Conceptualization, Validation, Visualization. **Ke Jin:** Formal analysis, Writing – orignal draft, Writing – review & editing. **Xin Yi:** Funding acquisition, Resources. **Zhaohui Dong:** Software. **Xun Guo:** Software, Writing – review & editing. **Ying Liu:** Methodology. **Yangyang Cheng:** Methodology, Resources. **Nannan Jia:** Writing – orignal draft. **Huiling Duan:** Funding acquisition. **Jianming Xue:**

Conceptualization, Supervision, Project administration, Writing – review & editing.

Declaration of Competing Interest

The authors declare that they have no known competing financial interests or personal relationships that could have appeared to influence the work reported in this paper.

Acknowledgments

This work is supported by the Science Challenge Project (No. TZ2018004), and National Natural Science Foundation of China (Grant No. 11632001, No. 11988102, No. 11521202, No. 11905008). We are grateful for computing resource provided by the High Performance Computing Platform of the Center for Life Science of Peking University, Weiming No. 1, Life Science No. 1 and Life Science Center High Performance Computing Platform at Peking University.

Appendix A. Supporting information

Supplementary data associated with this article can be found in the online version at doi:10.1016/j.jallcom.2021.162043.

References

[1] S.J. Zinkle, G.S. Was, Materials challenges in nuclear energy, Acta Mater. 61 (3) (2013) 735–758, https://doi.org/10.1016/j.actamat.2012.11.004
[2] C. Lu, T. Yang, K. Jin, N. Gao, P. Xiu, Y. Zhang, F. Gao, H. Bei, W.J. Weber, K. Sun, Y. Dong, L. Wang, Radiation-induced segregation on defect clusters in single-phase concentrated solid-solution alloys, Acta Mater. 127 (2017) 98–107, https://doi.org/10.1016/j.actamat.2017.01.019
[3] D.B. Miracle, O.N. Senkov, A critical review of high entropy alloys and related concepts, Acta Mater. 122 (2017) 448–511, https://doi.org/10.1016/j.actamat.2016.08.081
[4] J.-W. Yeh, S.-K. Chen, S.-J. Lin, J.-Y. Gan, T.-S. Chin, T.-T. Shun, C.-H. Tsau, S.-Y. Chang, Nanostructured high-entropy alloys with multiple principal elements: novel alloy design concepts and outcomes, Adv. Eng. Mater. 6 (5) (2004) 299–303, https://doi.org/10.1002/adem.2003005672004
[5] F. Granberg, K. Nordlund, M.W. Ullah, K. Jin, C. Lu, H. Bei, L.M. Wang, F. Djurabekova, W.J. Weber, Y. Zhang, Mechanism of radiation damage reduction in equiatomic multicomponent single phase alloys, Phys. Rev. Lett. 116 (13) (2016) 135504, https://doi.org/10.1103/PhysRevLett.116.135504 ⟨https://www.ncbi.nlm.nih.gov/pubmed/27081990⟩.
[6] O. El-Atwani, N. Li, M. Li, A. Devearaj, J.k.S. Baldwin, M.M. Schneider, D. Sobieraj, J.S. Wroble, D. Nguyen-Manh, S.A. Maloy, E. Martinez, Outstanding radiation resistance of tungsten-based high-entropy alloys, Sci. Adv. 5 (2019).
[7] Y. Lu, Y. Dong, H. Jiang, Z. Wang, Z. Cao, S. Guo, T. Wang, T. Li, P.K. Liaw, Promising properties and future trend of eutectic high entropy alloys, Scr. Mater. 187 (2020) 202–209, https://doi.org/10.1016/j.scriptamat.2020.06.022
[8] M. Wang, Y. Lu, T. Wang, C. Zhang, Z. Cao, T. Li, P.K. Liaw, A novel bulk eutectic high-entropy alloy with outstanding as-cast specific yield strengths at elevated temperatures, Scr. Mater. 204 (2021), https://doi.org/10.1016/j.scriptamat.2021.114132
[9] M.-R. He, S. Wang, S. Shi, K. Jin, H. Bei, K. Yasuda, S. Matsumura, K. Higashida, I.M. Robertson, Mechanisms of radiation-induced segregation in crfeconi-based single-phase concentrated solid solution alloys, Acta Mater. 126 (2017) 182–193, https://doi.org/10.1016/j.actamat.2016.12.046
[10] S.Q. Xia, X. Yang, T.F. Yang, S. Liu, Y. Zhang, Irradiation resistance in al x cocrfeni high entropy alloys, Jom 67 (10) (2015) 2340–2344, https://doi.org/10.1007/s11837-015-1568-4
[11] C. Lu, T. Yang, K. Jin, G. Velisa, P. Xiu, M. Song, Q. Peng, F. Gao, Y. Zhang, H. Bei, W.J. Weber, L. Wang, Enhanced void swelling in nicofecrpd high-entropy alloy by indentation-induced dislocations, Mater. Res. Lett. 6 (10) (2018) 584–591, https://doi.org/10.1080/21663831.2018.1504136
[12] N.A.P.K. Kumar, C. Li, K.J. Leonard, H. Bei, S.J. Zinkle, Microstructural stability and mechanical behavior of fenimncr high entropy alloy under ion irradiation, Acta Mater. 113 (2016) 230–244, https://doi.org/10.1016/j.actamat.2016.05.007
[13] K. Jin, W. Guo, C. Lu, M.W. Ullah, Y. Zhang, W.J. Weber, L. Wang, J.D. Poplawsky, H. Bei, Effects of fe concentration on the ion-irradiation induced defect evolution and hardening in ni-fe solid solution alloys, Acta Mater. 121 (2016) 365–373, https://doi.org/10.1016/j.actamat.2016.09.025
[14] W.-Y. Chen, X. Liu, Y. Chen, J.-W. Yeh, K.-K. Tseng, K. Natesan, Irradiation effects in high entropy alloys and 316h stainless steel at 300 °C, J. Nucl. Mater. 510 (13) (2018) 421–430, https://doi.org/10.1016/j.jnucmat.2018.08.031
[15] Y. Lu, H. Huang, X. Gao, C. Ren, J. Gao, H. Zhang, S. Zheng, Q. Jin, Y. Zhao, C. Lu, T. Wang, T. Li, A promising new class of irradiation tolerant materials: Ti2ZrHfv0.5Mo0.2 high-entropy alloy, J. Mater. Sci. Technol. 35 (3) (2019) 369–373, https://doi.org/10.1016/j.jmst.2018.09.034
[16] M. Sadeghilaridjani, A. Ayyagari, S. Muskeri, V. Hasannaeimi, R. Salloom, W.-Y. Chen, S. Mukherjee, Ion irradiation response and mechanical behavior of reduced activity high entropy alloy, J. Nucl. Mater. 529 (2020), https://doi.org/10.1016/j.jnucmat.2019.151955
[17] Y. Wang, K. Zhang, Y. Feng, Y. Li, W. Tang, B. Wei, Evaluation of radiation response in cocrfecuni high-entropy alloys, Entropy 20 (11) (2018), https://doi.org/10.3390/e20110835
[18] S. Sinha, R.A. Mirshams, T. Wang, S.S. Nene, M. Frank, K. Liu, R.S. Mishra, Nanoindentation behavior of high entropy alloys with transformation-induced plasticity, Sci. Rep. 9 (1) (2019) 6639, https://doi.org/10.1038/s41598-019-43174-x ⟨https://www.ncbi.nlm.nih.gov/pubmed/31036887⟩.
[19] H.F. Huang, J.J. Li, D.H. Li, R.D. Liu, G.H. Lei, Q. Huang, L. Yan, Tem, xrd and nanoindentation characterization of xenon ion irradiation damage in austenitic stainless steels, J. Nucl. Mater. 454 (1–3) (2014) 168–172, https://doi.org/10.1016/j.jnucmat.2014.07.033
[20] D. Kiener, P. Hosemann, S.A. Maloy, A.M. Minor, In situ nanocompression testing of irradiated copper, Nat. Mater. 10 (8) (2011) 608–613, https://doi.org/10.1038/nmat3055 ⟨https://www.ncbi.nlm.nih.gov/pubmed/21706011⟩.
[21] Z.W. Shan, R.K. Mishra, S.A. SyedAsif, O.L. Warren, A.M. Minor, Mechanical annealing and source-limited deformation in submicrometre-diameter ni crystals, Nat. Mater. 7 (2) (2008) 115–119, https://doi.org/10.1038/nmat2085 ⟨https://www.ncbi.nlm.nih.gov/pubmed/18157134⟩.
[22] Y. Zou, H. Ma, R. Spolenak, Ultrastrong ductile and stable high-entropy alloys at small scales, Nat. Commun. 6 (2015) 7748, https://doi.org/10.1038/ncomms8748 ⟨https://www.ncbi.nlm.nih.gov/pubmed/26159936⟩.
[23] I. Ryu, W.D. Nix, W. Cai, Plasticity of bcc micropillars controlled by competition between dislocation multiplication and depletion, Acta Mater. 61 (9) (2013) 3233–3241, https://doi.org/10.1016/j.actamat.2013.02.011
[24] C. Li, X. Hu, T. Yang, N.A.P.K. Kumar, B.D. Wirth, S.J. Zinkle, Neutron irradiation response of a co-free high entropy alloy, J. Nucl. Mater. 527 (2019), https://doi.org/10.1016/j.jnucmat.2019.151838
[25] D. Cáceres, I. Vergara, R. González, Y. Chen, Effect of neutron irradiation on hardening in mgo crystals, Phys. Rev. B 66 (2) (2002), https://doi.org/10.1103/PhysRevB.66.024111
[26] P. Litwa, L. Kurpaska, R.A. Varin, K. Perkowski, J. Jagielski, S. Jóźwiak, T. Czujko, The effect of he. irradiation on hardness and elastic modulus of fe-cr-40 wt% tib 2 composite rod designed for neutron absorbing, J. Alloy. Compd. 711 (2017) 111–120, https://doi.org/10.1016/j.jallcom.2017.03.350
[27] G.S. Was, J.T. Busby, T. Allen, E.A. Kenik, A. Jenssen, S.M. Bruemmer, J. Gan, A.D. Edwards, P.M. Scott, P.L. Andresen, Emulation of neutron irradiation effects with protons: validation of principle, J. Nucl. Mater. 300 (2002) 198–216.
[28] Q. Dong, H. Qin, Z. Yao, M.R. Daymond, Irradiation damage and hardening in pure zr and zr-nb alloys at 573 k from self-ion irradiation, Mater. Des. 161 (2019) 147–159, https://doi.org/10.1016/j.matdes.2018.11.017
[29] M. Zhao, F. Liu, Z. Yang, Q. Xu, F. Ding, X. Li, H. Zhou, G.-N. Luo, Fluence dependence of helium ion irradiation effects on the microstructure and mechanical properties of tungsten, Nucl. Instrum. Methods Phys. Res. Sect. B: Beam Interact. Mater. At. 414 (2018) 121–125, https://doi.org/10.1016/j.nimb.2017.09.002
[30] K. Yabuuchi, Y. Kuribayashi, S. Nogami, R. Kasada, A. Hasegawa, Evaluation of irradiation hardening of proton irradiated stainless steels by nanoindentation, J. Nucl. Mater. 446 (1–3) (2014) 142–147, https://doi.org/10.1016/j.jnucmat.2013.12.009
[31] X. Liu, R. Wang, A. Ren, J. Jiang, C. Xu, P. Huang, W. Qian, Y. Wu, C. Zhang, Evaluation of radiation hardening in ion-irradiated fe based alloys by nanoindentation, J. Nucl. Mater. 444 (1–3) (2014) 1–6, https://doi.org/10.1016/j.jnucmat.2013.09.026
[32] Y. Cui, E. Aydogan, J.G. Gigax, Y. Wang, A. Misra, S.A. Maloy, N. Li, In situ micropillar compression to examine radiation-induced hardening mechanisms of fecral alloys, Acta Mater. 202 (2021) 255–265, https://doi.org/10.1016/j.actamat.2020.10.047